

We are IntechOpen, the world's leading publisher of Open Access books Built by scientists, for scientists

4,800

Open access books available

122,000

International authors and editors

135M

Downloads

Our authors are among the

154

Countries delivered to

TOP 1%

most cited scientists

12.2%

Contributors from top 500 universities



WEB OF SCIENCE™

Selection of our books indexed in the Book Citation Index
in Web of Science™ Core Collection (BKCI)

Interested in publishing with us?
Contact book.department@intechopen.com

Numbers displayed above are based on latest data collected.
For more information visit www.intechopen.com



Imaging the Cornea, Anterior Chamber, and Lens in Corneal and Refractive Surgery

Timo Eppig, Stephanie Mäurer, Loay Daas,
Berthold Seitz and Achim Langenbucher

Additional information is available at the end of the chapter

<http://dx.doi.org/10.5772/intechopen.78293>

Abstract

Anterior segment OCT (AS-OCT) is an optical and noncontact imaging technology, which has numerous fields of application in the imaging of the cornea, anterior chamber, and the lens. In this chapter, we will present some of the application fields of AS-OCT in corneal, cataract, and refractive surgery. We will emphasize the potential of AS-OCT by several clinical examples including corneal imaging (keratoconus, keratoplasty, and refractive surgery) and intraocular lens imaging after refractive surgery. AS-OCT shows special potential for corneal imaging in case of corneal edema and for postoperative control after Descemet's membrane endothelial keratoplasty (DMEK). The postoperative follow-up of a posterior chamber Collamer lens's vault and measuring the anterior chamber angle could be identified as another promising field of application for AS-OCT.

Keywords: anterior segment, cataract, refractive surgery, cornea, keratoplasty, keratoconus, intracorneal ring segments, LASIK, phakic intraocular lenses

1. Introduction

Since its development in the late 1980s, optical coherence tomography (OCT) has found numerous applications not only in ophthalmology. The first ophthalmological applications were tomographical imaging of the ultrastructure of the human retina, especially the fovea. For the first time OCT allowed tomographic imaging of the retinal layers allowing detection of subretinal changes and high precision assessment of the changes in retinal nerve fiber layer thickness. The visible to near infrared wavelengths used in posterior segment OCT devices

allowed high transmission in aqueous material and high reflectivity at retinal structures. At that time, the Scheimpflug imaging technology was able to provide high resolution tomographic images of the anterior segment including the lens [1]. Anterior segment biometry, such as measuring corneal thickness (pachymetry) and the depth of the anterior chamber for surgery planning in corneal refractive surgery or calculating intraocular lenses (IOL) could only be performed by ultrasound biomicroscopy or Scheimpflug imaging [2, 3]. In the 1990s, the leading research groups in OCT technology presented the first results in anterior segment imaging and biometry [4–6]. Dedicated OCT devices for tomographic imaging of the anterior segment (AS-OCT) were not available until Zeiss Meditec launched their Visante™ 1000 OCT which was based on time domain OCT technology [3]. In 2009, Tomey launched their swept-source based OCT Casia SS-1000, which was also dedicated to anterior segment imaging. Manufacturers of posterior segment OCT devices soon provided additional objective lenses allowing tomographic imaging of anterior segment structures. During the last decade, the OCT technology conquered numerous applications including corneal imaging, refractive surgery, lens imaging, glaucoma, and cataract surgery.

In this chapter, we will present and discuss applications of OCT technology in the imaging of the anterior segment of the human eye, including general imaging of anterior segment morphology as well as applications in corneal and anterior segment surgery.

2. Cornea

The cornea is the most outer structure of the human eye and contributes to about $2/3$ ($=48$ D) of the total optical power to the eye. The cornea's structure can be subdivided into six layers with the epithelium (EP) being the outer layer which covers Bowman's layer (BL). The epithelium is covered by the tear film and consists of up to six layers of epithelial cells. Its average thickness is about $50\ \mu\text{m}$. Bowman's layer is a collagenous, acellular, nonregenerating layer and separates the epithelial cell layer from the stroma. The stroma covers 85% of the volume in the human cornea with a total thickness of about $350\text{--}450\ \mu\text{m}$ [7]. The posterior limitation of the stroma is Descemet's membrane (DM), which has a thickness of about $10\text{--}15\ \mu\text{m}$ [7]. The DM is the basal membrane for the endothelial cell layer, which is a single-layer of hexagonal endothelial cells with a thickness of about $4.5\ \mu\text{m}$. Dua et al. [7] identified an additional pre-Descemetal layer of $10\text{--}15\ \mu\text{m}$ thickness, which they named Dua's layer (DL).

The different layers of the human cornea can be imaged *in vivo* by specialized ultrahigh-resolution OCT systems as shown by Werkmeister et al. [8] (**Figure 1**).

2.1. Keratoconus

Keratoconus (KC) is a corneal disease characterized by a progressive steepening and protrusion of the corneal topography accompanied by a central to paracentral thinning (**Figure 2**). Keratoconus is a bilateral disease and often manifests within the second to third decade of life. Primary diagnosis is being supported by corneal topography and corneal tomography, which both can be performed by AS-OCT. AS-OCT assists in early detection and monitoring of the progression of

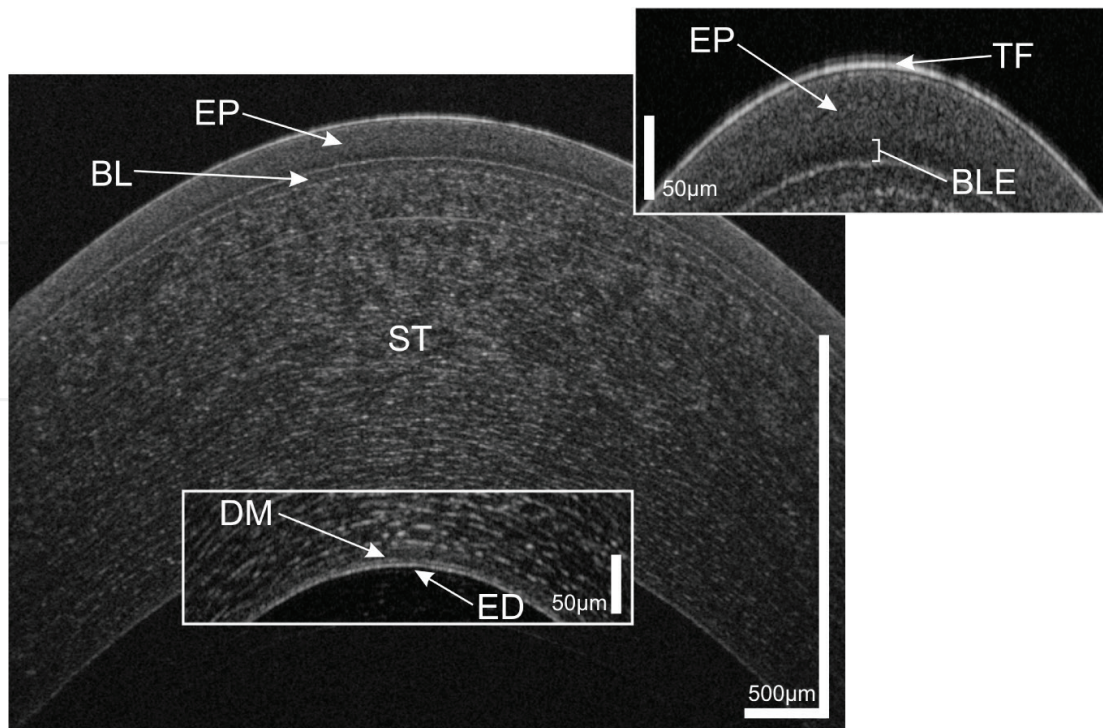


Figure 1. UHR-OCT tomogram of the central and paracentral zone of the cornea of a 38-year-old healthy male. TF, tear film; EP, epithelium; BLE, basal layer of epithelium; BL, Bowman's layer; ST, corneal stroma; DM, Descemet's membrane; ED, endothelium. Reprinted with permission from Werkmeister et al. [8], © Optical Society of America.

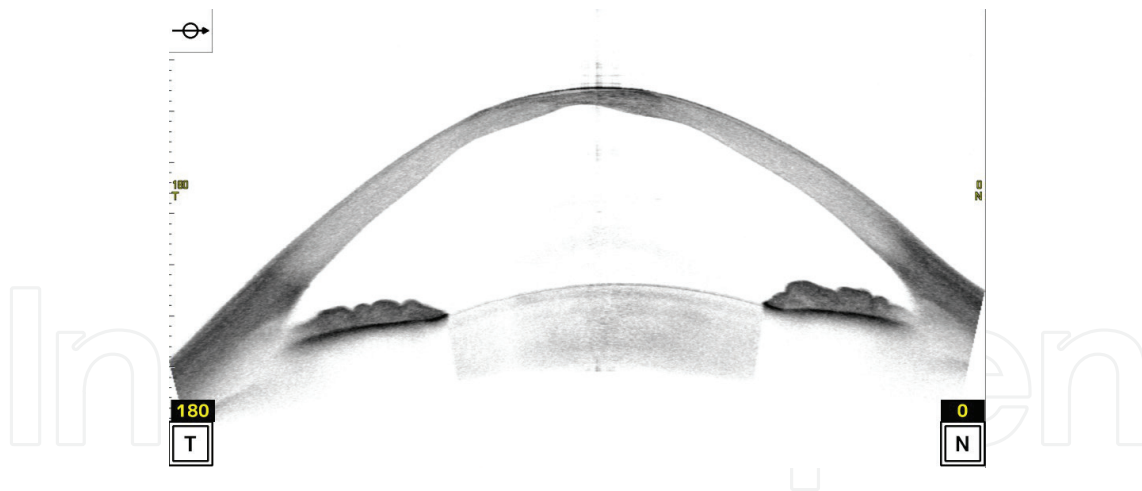


Figure 2. Horizontal image slice of an eye with keratoconus especially notable at the posterior corneal surface. Image taken with Casia 2 AS-OCT (Tomey Corp., Nagoya, Japan).

the disease in order to provide stage oriented therapeutic options. The high reliability of corneal thickness measurements make AS-OCT a useful tool for monitoring changes in corneal thickness, however measurements could not be used interchangeably with other modalities such as Scheimpflug imaging [9–11]. Schröder et al. have shown that AS-OCT technology provides a high repeatability for measuring the corneal thickness in healthy patients. They also showed that the posterior surface measurement was more reliable than with Scheimpflug technology [11].

New methods such as corneal OCT and topographic mapping of EP and BL have been proposed for early detection of keratoconus [12–15]. However, this requires high-resolution OCT technology in order to resolve EP and BL with sufficient precision.

In late, advanced stages of keratoconus, DM may tear allowing the aqueous humor to penetrate the stroma. This situation is also known as acute keratoconus, which is characterized by a corneal edema and opacification (corneal hydrops). The edema limits the visibility of structures in the anterior chamber. The development of the Descemet's tear may differ between patients, and AS-OCT is able to image through the corneal edema allowing the examiner to locate the Descemet's tear (**Figure 3**). Scheimpflug technology is limited in these cases due to increased light scattering. After the edema has diminished, the Descemet tear usually cicatrizes, affecting the patient's visual acuity. The ultimate therapeutic option is penetrating keratoplasty (PK). However, from the surgeon's point of view, the hydrops should resolve before PK should be performed [16]. AS-OCT is an ideal method for staging the disease and documenting the course of corneal hydrops (**Figure 4**) in order to define the time point when PK may be performed [17]. Pre-Descemetal sutures may be used to assist the edema in resolving and the DM in reattaching to the stroma. Therefore, the corneal hydrops is being sutured perpendicular to the DM tear [18]. Re-attachment of DM is being supported by an intracameral air bubble [18]. Despite impaired insight into the anterior chamber, AS-OCT allows taking a nearly unobstructed tomographic image of the anterior chamber including visualization of the DM tear facilitating suture planning prior to surgery [18].

In early stages of KC, when DM is unaffected and scarring has occurred in the stroma only, a deep anterior lamellar keratoplasty (DALK) may be a useful option. In this case, only the stroma (without DM) is being transplanted. AS-OCT may help to visualize pre-Descemetal scarring in order to check patients' eligibility for DALK. The utility of intraoperative AS-OCT has been proven for analyzing whether the diseased stroma has been fully removed and whether the transplant has been well integrated into the host tissue [19, 20]. In the follow-up AS-OCT again is useful to check the graft adhesion to the host's DM or to visualize DM and the anterior chamber if the view is limited due to increased light scatter caused by corneal edema (**Figure 5**). Again, OCT allows a detailed a tomographic view of the host-graft interface, which usually exhibits a high amount of scattered light.

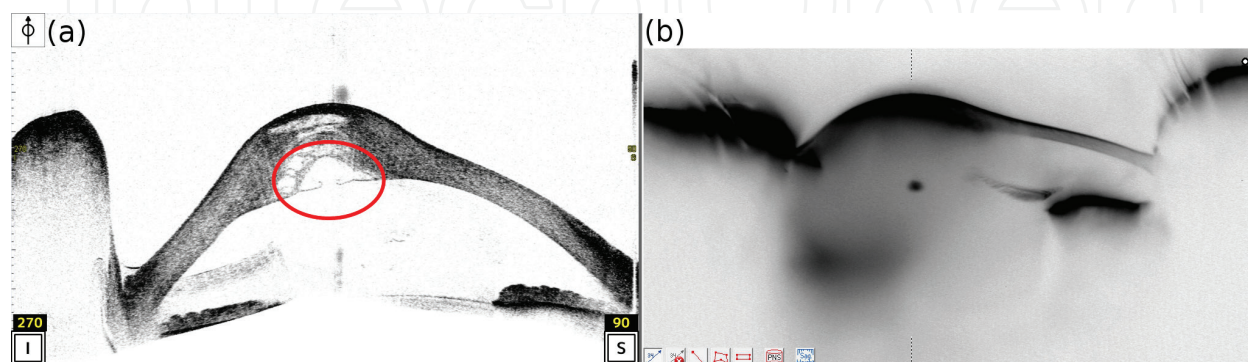


Figure 3. Eye of a 25-year-old patient with acute keratoconus (corneal hydrops). (a) The AS-OCT (Casia 2, Tomey Corp., Nagoya, Japan) image reveals the extent of the corneal edema and the location of the Descemet's rupture. The Descemet's membrane rolls are clearly visible indicating the strain of Descemet's membrane. (b) Scheimpflug imaging (Pentacam® HR, Oculus Optikgeräte GmbH, Wetzlar) is limited and cannot image the anterior chamber due to increased light scattering.

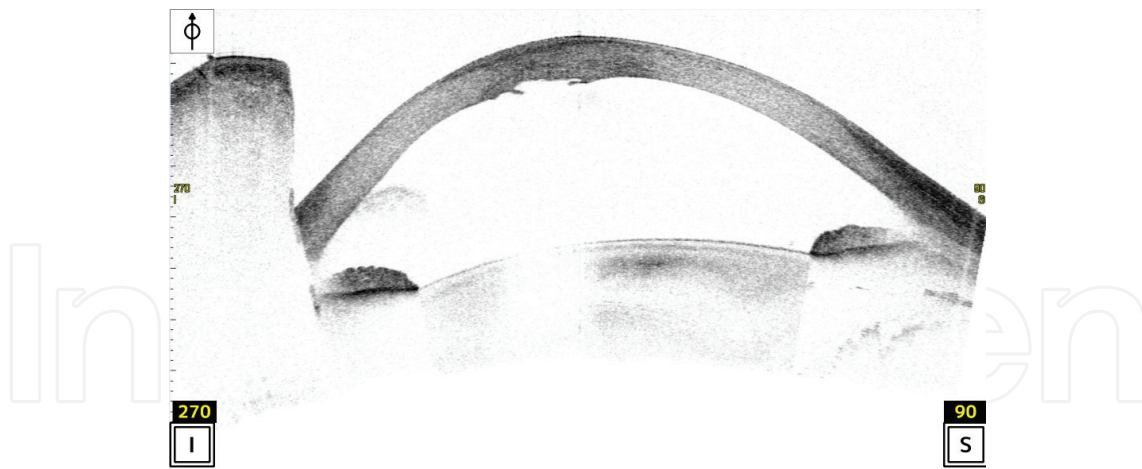


Figure 4. Eye of a 25-year-old patient 3 months after acute keratoconus (**Figure 3**) that had been treated with Muraine sutures and an air bubble in the anterior chamber. The corneal edema widely disappeared leaving a central scar including the posterior surface. The opacification is still present, visible as darker stroma in the center. Image taken with Casia 2 AS-OCT (Tomey Corp., Nagoya, Japan).



Figure 5. Descemet's rupture during DALK surgery with major edema of the full-thickness graft. Image taken with Casia SS-1000 AS-OCT (Tomey Corp., Nagoya, Japan).

2.2. Refractive surgery

The high axial resolution of AS-OCT and the capability of detecting small changes in reflectivity are ideal prerequisites for applications in corneal refractive surgery. AS-OCT is capable of imaging corneal incisions, scars, and flaps created during laser in-situ keratomileusis (LASIK). It can be used as diagnostic tool for measuring the pre- to postoperative change in corneal thickness as well as for controlling the flap thickness and flap quality. **Figure 6** shows an eye with femtosecond-laser-assisted LASIK (fs-LASIK) with a flap thickness of 120 μm . An eye with microkeratome-created LASIK-flap 18 years after surgery is shown in **Figure 7** revealing a residual stromal bed thickness of about 300 μm . AS-OCT can also assist in identifying the causes for post-LASIK corneal ectasia as shown in **Figure 8**, where we could detect a misbalanced ratio of flap to stromal bed thickness and a too thin residual stromal bed.

New methods such as small incision lenticule extraction (SMILE) could also be visualized with AS-OCT [21]. Intraoperative AS-OCT was shown to be useful in visualizing the lenticule during the management of complications in SMILE surgery [22, 23].

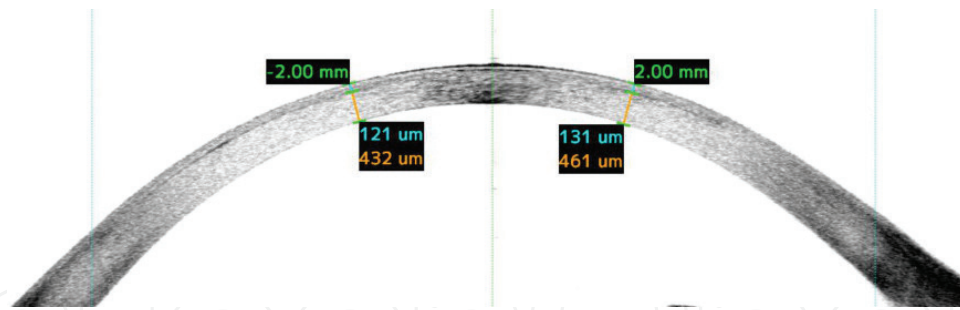


Figure 6. Right eye of a patient having received femtosecond-laser-assisted LASIK. The flap thickness of about 120 μm could be measured with the AS-OCT (Casia 2, Tomey Corp., Nagoya, Japan).

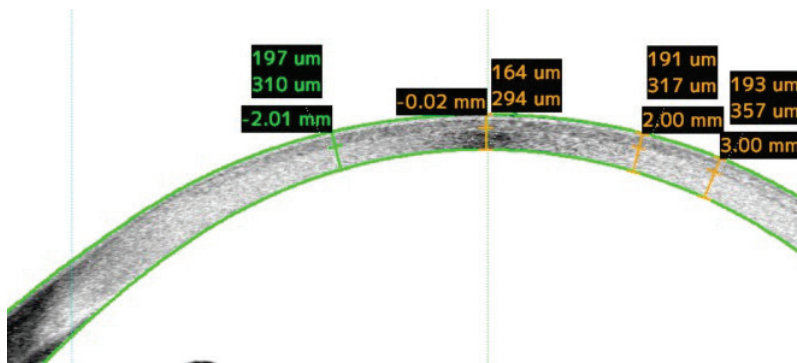


Figure 7. Left eye of a 39-year-old male with a microkeratome-created LASIK flap, which is still visible 18 years after surgery. The thickness values provided are separated into flap thickness and stromal bed thickness. The residual stromal bed is around 300 μm . Image taken with Casia 2 AS-OCT (Tomey Corp., Nagoya, Japan).

Intracorneal ring segments (ICRS) are an option for reducing the refractive power of the cornea in keratoconus if the optical center is free from scars. Therefore, a circular tunnel is being prepared within the stroma into which the plastic ring(s) are being implanted. The tunnel may be prepared mechanically or with a femtosecond-laser. However, Monteiro et al. have shown with AS-OCT that femtosecond-laser based tunnel preparation is more predictable than manual tunnel preparation [24]. Currently, there are various ICRS models on the market with different cross-sectional geometry, thickness, and arc lengths. The thickness, arc length and implantation site is usually defined by proprietary nomograms [25]. In the follow-up of ICRS, AS-OCT is useful for investigating proper placement of the ring segments, especially the distance to DM and/or BL and the epithelium [26]. In these cases, the plastic rings within the cornea will induce artifacts visible as bright stripes parallel to the line of sight. Structures lying behind these rings are subject to distortion due to the change of refractive index, which currently cannot be interpreted by clinical AS-OCT software. **Figure 9** shows an eye with intracorneal ring segments for keratoconus. Due to this image distortion, a reliable measurement of the thickness behind these structures is not feasible. However, AS-OCT is useful to follow relative changes or displacement of ICRS over time.

In patient's having received a corneal pinhole implant (KAMRA[®], Acufocus Inc., Irvine, USA), the centration and implantation of the implant beneath the femtosecond-laser-created flap is crucial and should be controlled in the OCT image. Due to the very prominent Purkinje reflex visible in the central OCT image, the assessment of proper KAMRA[®] implant centration could be performed at ease. However, the absorption of the pinhole implant hides any structures lying behind the implant (**Figure 10**).

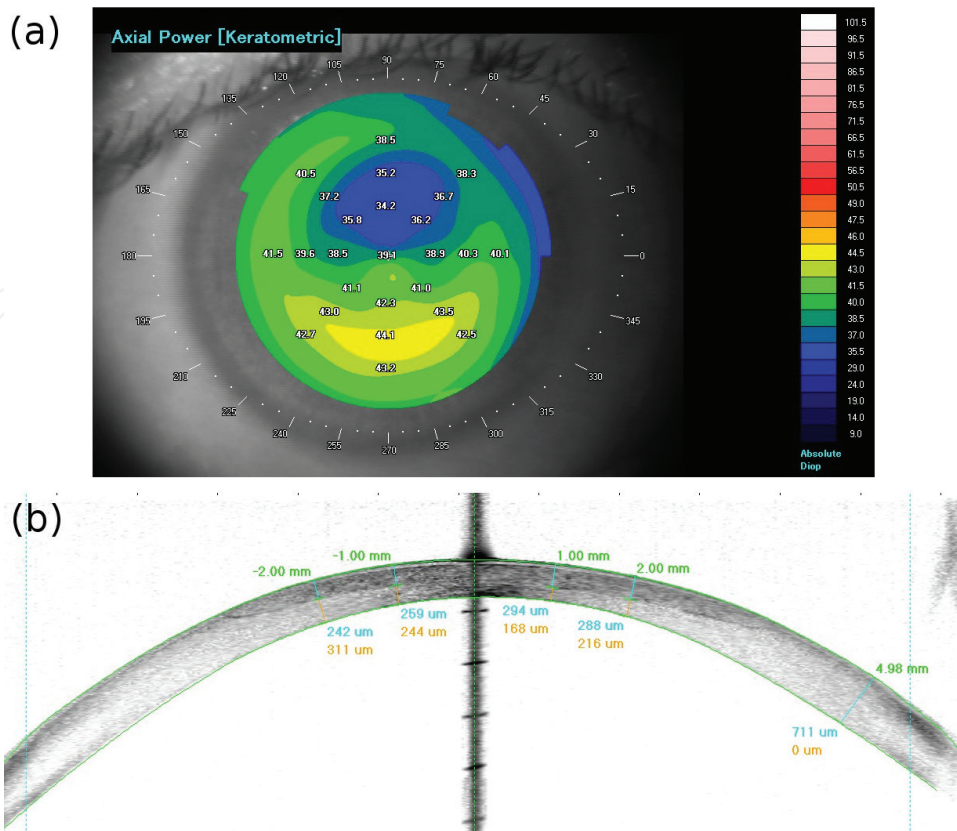


Figure 8. (a) AS-OCT-derived corneal topography in a 44-year-old patient some years after LASIK surgery. The topography reveals a decentered ablation and late onset of corneal ectasia. (b) The flap is clearly visible and the residual bed thickness was found to be less than 200 μm . Images taken with Casia SS-1000 AS-OCT (Tomey Corp., Nagoya, Japan).

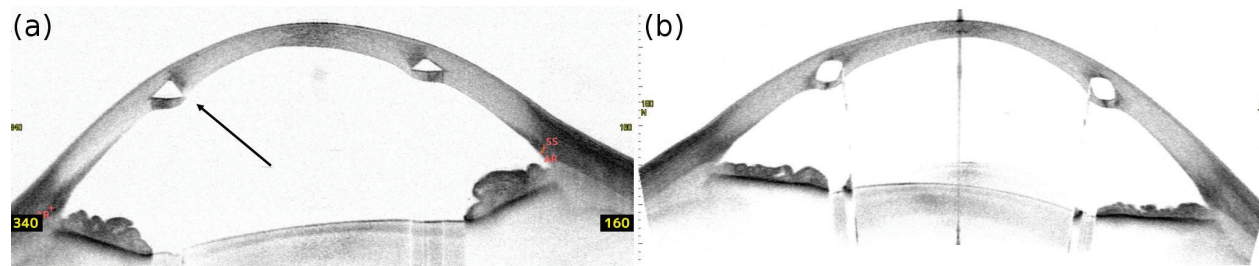


Figure 9. (a) Keratoconus eye with intracorneal ring segments (ICRS) with prismatic cross section. The sharp edge of the temporal ring (arrow) is close to the DM and should be monitored. (b) Cornea with femtosecond-laser-assisted Intacs® SK ICRS (Addition Technology Inc., Lombard, USA) implantation. The OCT image reveals the elliptic cross section of the Intacs® SK implants. The ICRS edge causes artifacts within the anterior chamber. Images taken with Casia 2 AS-OCT (Tomey Corp., Nagoya, Japan).

2.3. Corneal transplantation

The first successful transplantation of corneal tissue has been performed by Eduard Zirm in 1905 [27]. Since then, corneal transplantation has been the oldest and most successful technique of human tissue or organ transplantation. Starting from the original PK and the transfer of all corneal layers, new techniques such as lamellar transplantation have been emerging. PK has been proven to provide good optical results and excellent transplant survival depending on the initial indication for PK [28]. However, complications such as posterior step formation,

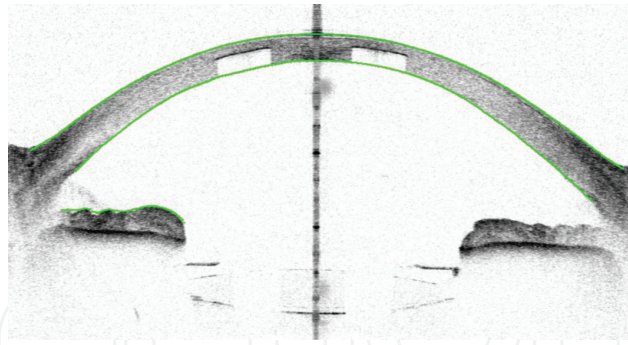


Figure 10. Pseudophakic eye with a KAMRA® intracorneal inlay for presbyopia treatment under a 200- μ m femtosecond-laser flap. The central Purkinje reflex reveals that both intraocular lens and corneal inlay are well centered. Image taken with Casia 2 AS-OCT (Tomey Corp., Nagoya, Japan).

graft opacification or graft rejection may occur. In addition, a partially irregular postoperative corneal astigmatism is one of the side effects of PK. Szentmáry et al. [29] showed that nonmechanical trephination during PK yields better morphological and functional results than mechanical trephination. The immunological drawbacks could be minimized by novel lamellar techniques such as DALK, Descemet's stripping automated endothelial keratoplasty (DSAEK) or Descemet membrane endothelial keratoplasty (DMEK) [16]. AS-OCT may help in assessing the graft adhesion, the host-graft interface [30], graft thickness or step formation [31]. Yenerel et al. argued that AS-OCT may be a useful tool in monitoring the morphological results of PK and in the management of the postoperative complications after PK [32]. **Figure 11** shows two eyes after excimer-laser and top-hat profile femtosecond-laser-assisted keratoplasty illustrating the different trephination techniques.

2.3.1. Descemet stripping automated endothelial keratoplasty (DSAEK)

Posterior lamellar keratoplasty was originally introduced by Melles in 1998 and had continuously been improved until 2004 when Melles presented a new method for stripping the DM which led to the Descemet stripping automated endothelial keratoplasty (DSAEK) procedure

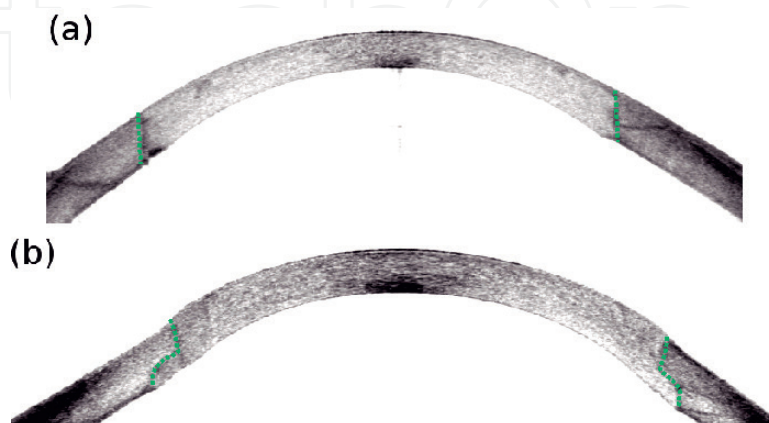


Figure 11. (a) Integrated graft in an eye after excimer-laser-assisted keratoplasty showing the straight interface and no step formation. (b) An eye after femtosecond-laser-assisted keratoplasty using a top-hat trephination profile. The dashed lines highlight the graft-host interface. Images taken with Casia 2 AS-OCT (Tomey Corp., Nagoya, Japan).

[33, 34]. The objective was to implement a technique for lamellar keratoplasty for the transplantation of endothelial cells leaving the host's stroma in place. A thin graft of DM and stroma is being prepared from donor tissue. After stripping the host's DM the graft is placed onto the posterior side of the host cornea. Intraoperative OCT may assist in the positioning of the graft [35, 36]. Due to the thickness and geometric profile of the graft, the posterior surface of the host cornea is changed causing a change in total corneal power (**Figure 12**). This leads to invalid keratometer readings and systematic errors in intraocular lens power calculations in DSAEK eyes, leading to a hyperopic shift of up to 1.5 D [37–39]. This has to be considered in intraocular lens calculation and requires adjustment in case of combined DSAEK and cataract surgery. Therefore, corneal tomography (either AS-OCT or Scheimpflug imaging) is mandatory in these cases. In case of sequential cataract surgery in DSAEK eyes AS-OCT and Scheimpflug imaging are useful tools to calculate the total corneal refractive power instead of keratometer readings [39].

2.3.2. Descemet's membrane endothelial keratoplasty (DMEK)

Descemet's membrane endothelial keratoplasty (DMEK) was originally proposed by Melles et al. in 2006 [40] and has been increasingly performed during the last decade [41]. The indications include endothelial diseases such as in Fuchs' dystrophy when the corneal edema affects corneal transparency and visual acuity. During surgery, the DM of the host is being stripped and replaced by a donor DM with healthy endothelium. Graft attachment to the host stroma is crucial and is usually supported by a gas bubble, which is intraoperatively injected into the anterior chamber. The adhesion of the graft requires monitoring during the first days and weeks after surgery. The high resolution of AS-OCT is essential for imaging small adhesion defects and to locate the dehiscence of the graft. Especially in the short term after surgery, patients should frequently be monitored by AS-OCT in order to document graft adhesion and to determine, whether a re-bubbling is required (**Figures 13** and **14**). AS-OCT examination outperforms slit-lamp examination in the short term DMEK monitoring and the examination is quick and more comfortable for the patients than slit-lamp examination. Therefore, a three-dimensional view of the anterior segment is beneficial (video 1). Eyes after DMEK are also subject to a hyperopic shift after IOL implantation. However, the change of total corneal refractive power is markedly smaller (about 0.5 D) in DMEK than in DSAEK [42, 43].

2.3.3. Screening of corneal donor tissue

Eye banks are in charge of checking eligibility of corneal donor tissue for PK. The analysis procedure includes visual inspection, morphological and microbiological examination. One crucial parameter is the endothelial cell density, which should exceed 2000 cells/mm². The stroma should be free from scars for good visual rehabilitation. Corneas from donors with keratoconus or that had undergone any laser refractive surgery should not be used for PK due to the unpredictable refractive result. However, the DM might be eligible for posterior lamellar keratoplasty such as DMEK. Keratoconic and postrefractive surgery corneas could be detected by analyzing the anterior and posterior radii of curvature and the corneal thickness profile or by detecting structural changes in the corneal tissue [44]. However, in-vivo data from donors are rarely available and therefore screening of donor tissue tomography could only be performed during tissue cultivation. OCT technology allows sterile, direct noncontact tomographic imaging of corneal donor

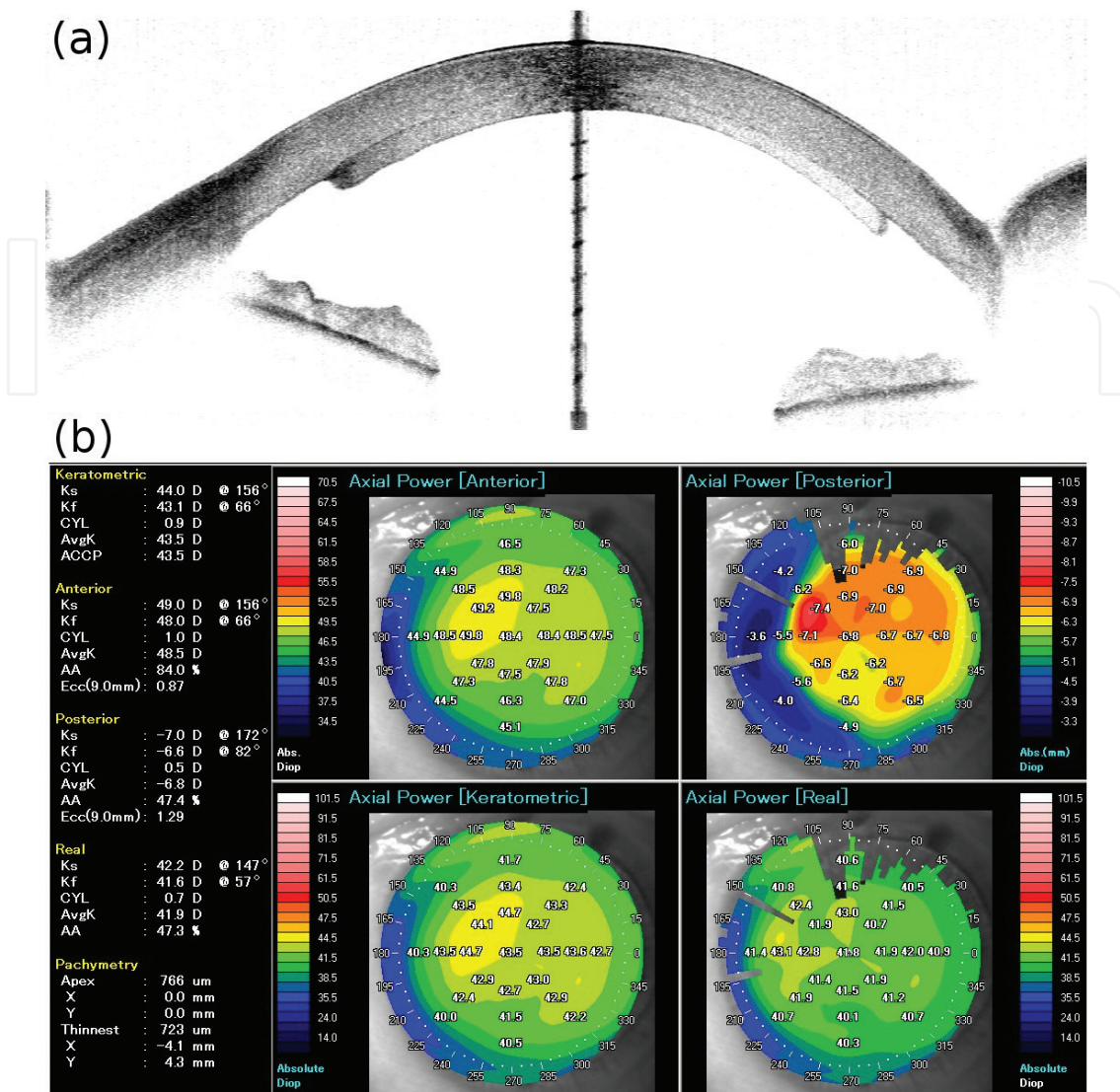


Figure 12. (a) Eye after DSAEK showing the graft well attached to the host stroma (Casia SS-1000 AS-OCT, Tomey Corp., Nagoya, Japan). The graft thickness was between 190 and 290 μ m. (b) Graphical representation of the anterior and posterior refractive power as well as the keratometric power and total refractive (real) power. The values indicate that using the keratometric power, the corneal power will be over-estimated by 1.6 D (average keratometric power 43.5 D vs. real corneal power 41.9 D), which would lead to hyperopic shift after cataract surgery.



Figure 13. Vertical cross-section of a pseudophakic eye after combined DMEK and cataract surgery showing a large superior dehiscence of the graft and a partially decompensated cornea, which requires rebubbling. Image taken with Casia 2 AS-OCT (Tomey Corp., Nagoya, Japan).

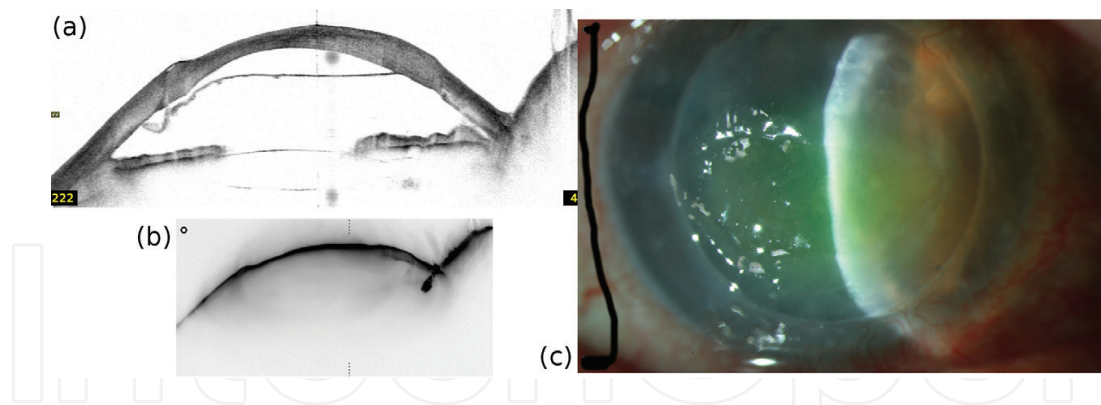


Figure 14. (a) Large area detachment of the graft after DMEK and cataract surgery. The cornea was fully opaque and (b) Scheimpflug imaging (Pentacam® HR, Oculus Optikgeräte GmbH, Wetzlar, Germany) or (c) slit-lamp examination (BX 900, Haag-Streit AG, Koeniz, Switzerland) of the anterior segment were impossible. The AS-OCT (Casia 2 AS-OCT, Tomey Corp., Nagoya, Japan) image, however, allowed analyzing the detached DM and anterior chamber.

tissue with the donor tissue placed within the culture flask. First attempts have been presented by Neubauer and Priglinger [45, 46] and the method has been enhanced with different devices and methods by Janunts et al. [47] (CASIA SS-1000, Tomey Corp., Nagoya, Japan) and Damian et al. (Spectralis Anterior Segment Module, Heidelberg Engineering GmbH, Heidelberg, Germany) [48].

Since the new AS-OCT Casia 2 (Tomey Corp., Nagoya, Japan) was launched to the market in 2016, we have developed an improved method for the tomographic screening of donor tissue. The culture flasks (Figure 15a) can be placed directly on the chin rest of the device (Figure 15c) and a volumetric scan allows capturing the complete corneal button including the holder (Figure 15b) to which the corneal button is attached while resting in the culture flask (Figure 16).

A custom written MATLAB® (The Mathworks, Natick, USA) script is then used to find the anterior and posterior surface of the corneal button in the volume dataset and a parametric surface model is fitted to the data allowing to calculate the radii of curvature and the thickness profile of the corneal button.

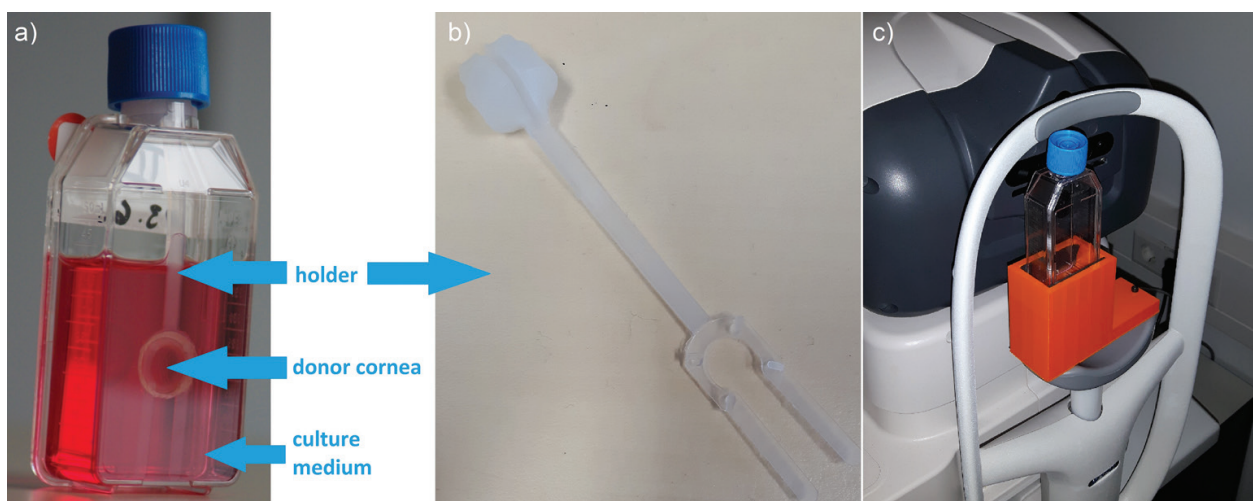


Figure 15. (a) Corneal tissue is cultivated within plastic culture flasks (adapted from Damian et al. [48], originally published under Creative Commons Attribution 3.0 Unported License. Available from: DOI:10.1117/1.JBO.22.1.016001). The corneal tissue is fixed in a holder (b) to avoid free floating of the tissue in the flask. (c) The culture flask is placed on the chin rest of the Casia 2 AS-OCT with a custom made 3D-printed adaptor.

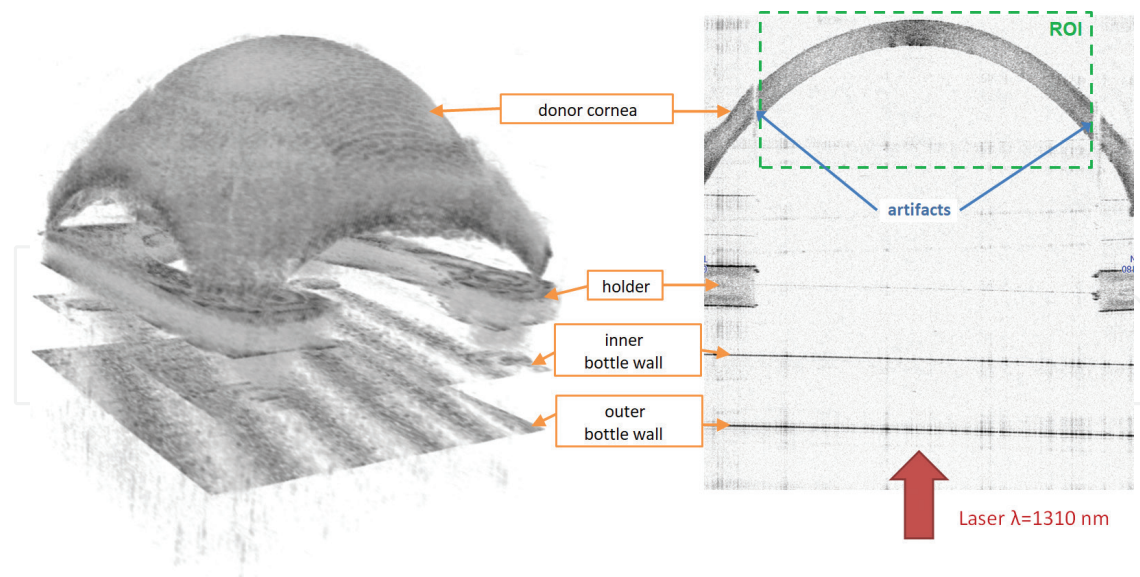


Figure 16. Volumetric dataset and central image slice from a donor cornea measured within the culture flask. The flask walls and the cornea holder are clearly visible in the image. The corneal radii of curvature can be calculated within a region of interest (ROI).

3. Phakic intraocular lenses

Precise assessment of the anterior chamber is important in glaucoma as well as in refractive surgery. Especially new concepts for refractive surgery require additional attention, such as phakic intraocular lenses. Posterior chamber implantable Collamer lenses (ICL) are a viable option for refractive surgery when corneal laser surgery is contraindicated. The most frequently used product of this type is the Visian[®] ICL. Such lenses are being implanted into the ciliary sulcus between the crystalline lens and the iris. The diameter of the lens has to be adapted to ciliary sulcus dimensions. The space could be estimated by using the diameter of the cornea (white-to-white diameter). Another option incorporates the use of ultrasound biomicroscopy to measure the diameter of the ciliary sulcus. The most frequent complications of early models of the ICL were a postoperative rise of intraocular pressure, angle closure, and cataract formation [49–51]. Therefore, the later models incorporated two holes within the plate haptic providing a bypass for the aqueous humor into the anterior chamber. The most recent type of ICL, the Visian[®] ICL V4c incorporates an additional hole in the center of the optic.

The size of the ICL is crucial to avoid contact of the ICL to the crystalline lens, which would typically happen with an undersized ICL. Oversized ICLs instead get vaulted toward the anterior chamber and may cause angle closure glaucoma [52]. Therefore, the distance of the posterior surface of the ICL to the anterior surface of the crystalline lens, the so called vault, is a key parameter to be monitored after ICL implantation. The feasibility of measuring the lens vault with AS-OCT was first shown by Bechmann et al. [53]. Several researchers reported the ICL vault to be within 90 μm and 1 mm, whereas an ideal vault is considered to be 0.5 mm [54–57]. Nakamura et al. [56] reported a method for ICL size calculation based on AS-OCT. Zhang et al. [58] compared anterior segment parameters measured with AS-OCT and ultrasound biomicroscopy. They found that AS-OCT slightly overestimated the vault and that both

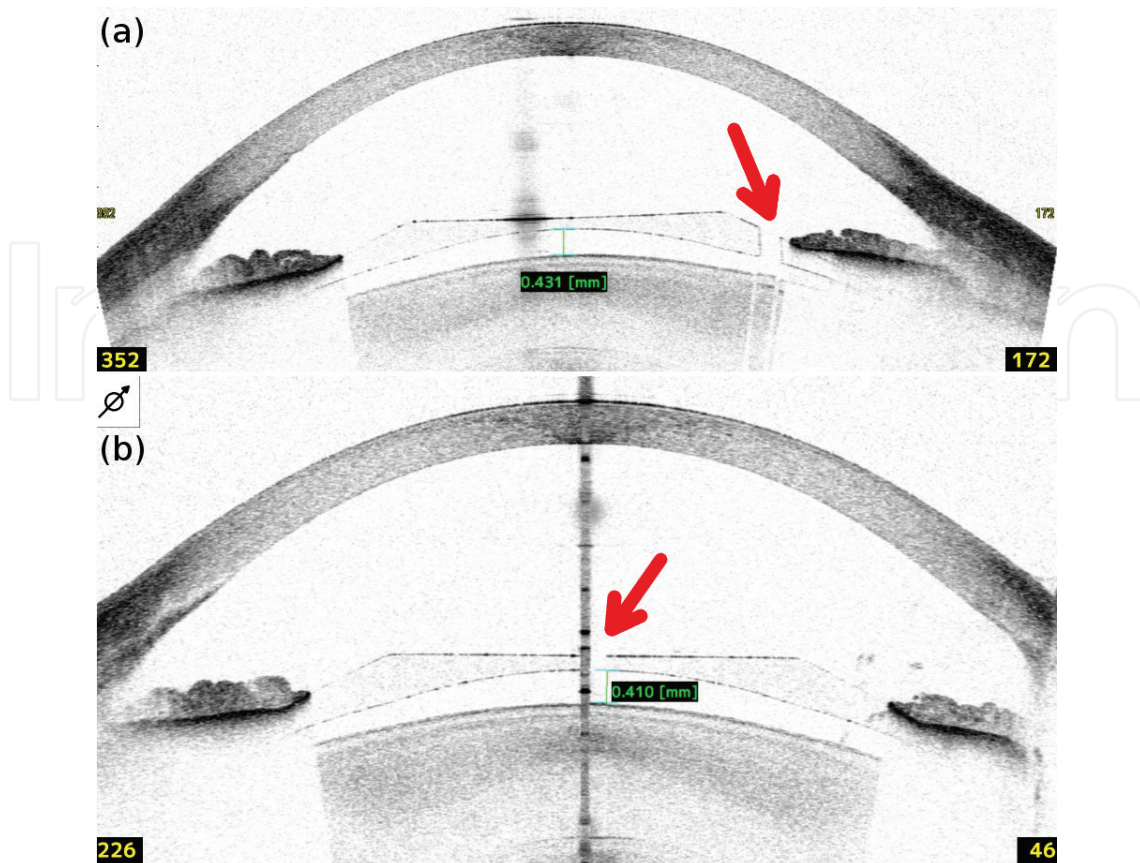


Figure 17. A myopic eye with a well-centered Visian[®] ICL V4c. The vault of the lens was larger than 400 μm in the center. The peripheral (top) and central (bottom) Aquaports are visible in separate image slices.

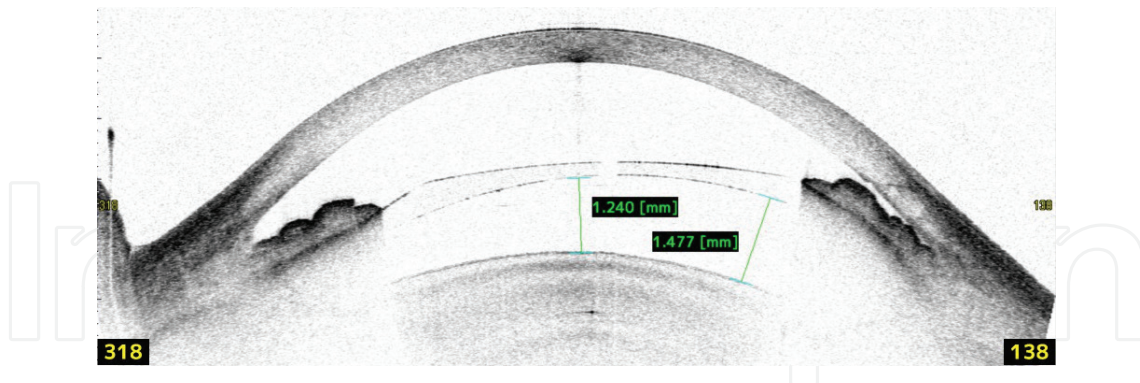


Figure 18. Angle closure at 138° after implantation of an oversized Visian[®] ICL V4c. The central Aquaport is visible in the image. The central vault is 1.2 mm and the peripheral vault up to 1.4 mm. Explantation of the ICL is recommended in order to prevent acute angle closure.

methods should not be used interchangeably. However, vault measurement requires manual interaction by an experienced operator as automatic analysis software is not available.

In addition, the anterior chamber angle (ACA) requires monitoring in order to detect early threat of angle closure. **Figure 17** shows a myopic eye with an ICL of the type Visian[®] V4c is shown in **Figure 17**, showing a well placed implant with two Aquaports and a wide ACA.

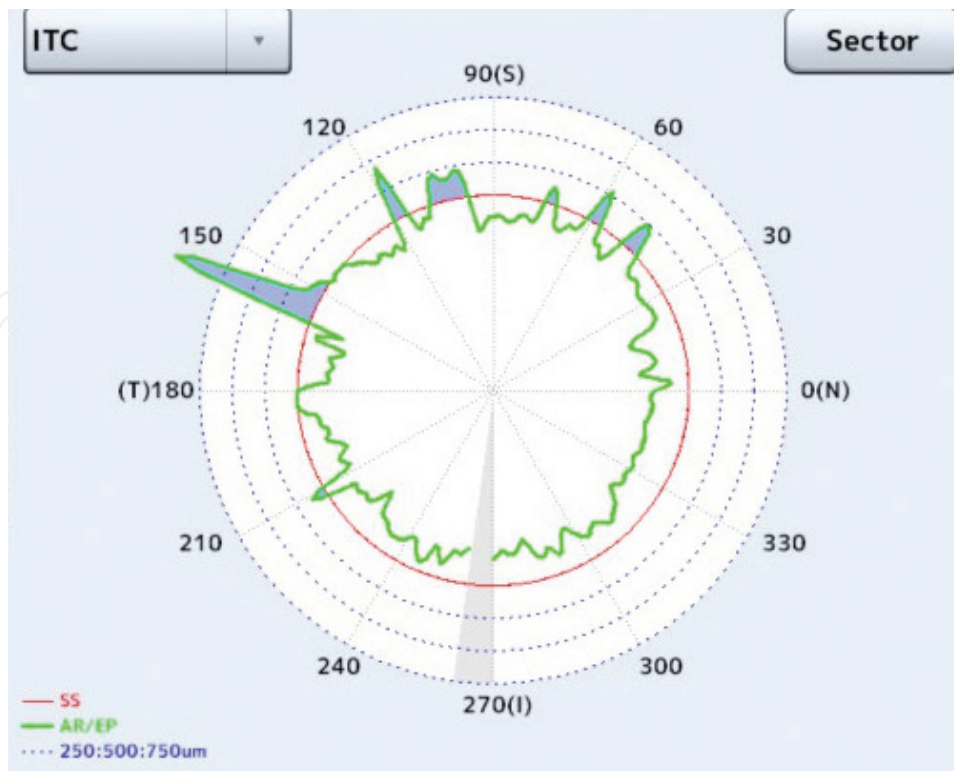


Figure 19. Star 360° analysis performed with the Casia 2 AS-OCT (Tomey Corp., Nagoya, Japan) on an eye with an oversized ICL (**Figure 18**). The green line touching the red circle and blue areas shows regions of angle closure within the circumference of the anterior chamber angle.

The application of AS-OCT in the follow-up after ICL implantation is emphasized by a case of a 26-year-old patient having undergone ICL implantation (Visian® ICL V4c) for myopia. We found a large and slightly asymmetric vault of the implant (**Figure 18**). An ACA analysis with the OCT's own software showed a threat of partial angle closure due to an oversized implant (**Figure 19**). Explantation of the ICL is recommended in order to prevent acute angle closure. The three-dimensional observation of the anterior chamber is essential.

4. Conclusions

Anterior segment OCT offers a variety of applications in corneal and refractive surgery, which need to be explored and enhanced in the future. Current analysis methods such as flap thickness or ICL vault require manual interaction by experienced operators in order to yield reproducible and representative results. The screening of corneal donor tissue allows retrieval of additional information on the tissue and may help to screen for anamnestically undetected refractive surgery such as LASIK or PRK.

Acknowledgements

The authors would like to acknowledge research funding by the Dr. Rolf M. Schwiete foundation for the development of the corneal donor screening methodology.

Conflict of interest

The authors have no conflict of interest to declare.

Appendices and nomenclature

ACA	anterior chamber angle
AS-OCT	anterior segment optical coherence tomography
D	diopter
DALK	deep anterior lamellar keratoplasty
DL	Dua's layer
DM	Descemet's membrane
DMEK	Descemet membrane endothelial keratoplasty
DSAEK	Descemet stripping automated endothelial keratoplasty
fs-LASIK	femtosecond-laser-assisted laser in-situ keratomileusis
ICL	implantable Collamer lens
ICRS	intracorneal ring segment
IOL	intraocular lens
KC	keratoconus
LASIK	laser in-situ keratomileusis
PK	penetrating keratoplasty
PRK	photorefractive keratectomy
ROI	region of interest
SMILE	small incision lenticule extraction

Author details

Timo Eppig^{1*}, Stephanie Mäurer¹, Loay Daas², Berthold Seitz² and Achim Langenbucher¹

*Address all correspondence to: timo.eppig@uks.eu

¹ Institute of Experimental Ophthalmology, Saarland University, Homburg, Germany

² Department of Ophthalmology, Saarland University Medical Center UKS, Homburg, Germany

References

- [1] Wegener A, Laser H. Optische Schnittbild-Vermessung des vorderen Augenabschnittes nach Scheimpflug: Möglichkeiten und Grenzen - eine Übersicht. *Klinische Monatsblätter für Augenheilkunde*. 2001;**218**:67-77. DOI: 10.1055/s-2001-12248
- [2] Wolffsohn JS, Davies LN. Advances in anterior segment imaging. *Current Opinion in Ophthalmology*. 2007;**18**:32-38. DOI: 10.1097/ICU.0b013e328011550d
- [3] Konstantopoulos A, Hossain P, Anderson DF. Recent advances in ophthalmic anterior segment imaging: A new era for ophthalmic diagnosis? *The British Journal of Ophthalmology*. 2007;**91**:551-557. DOI: 10.1136/bjo.2006.103408
- [4] Drexler W, Baumgartner A, Findl O, Hitzenberger CK, Sattmann H, Fercher AF. Submicrometer precision biometry of the anterior segment of the human eye. *Investigative Ophthalmology and Visual Science*. 1997;**38**:1304-1313
- [5] Hoerauf H, Wirbelauer C, Scholz C, Engelhardt R, Koch P, Laqua H, Birngruber R. Slit-lamp-adapted optical coherence tomography of the anterior segment. *Graefe's Archive for Clinical and Experimental Ophthalmology*. 2000;**238**:8-18
- [6] Izatt JA, Hee MR, Swanson EA, Lin CP, Huang D, Schuman JS, Puliafito CA, Fujimoto JG. Micrometer-scale resolution imaging of the anterior eye in vivo with optical coherence tomography. *Archives of Ophthalmology*. 1994;**112**:1584-1589
- [7] Dua HS, Faraj LA, Said DG, Gray T, Lowe J. Human corneal anatomy redefined: A novel pre-Descemet's layer (Dua's layer). *Ophthalmology*. 2013;**120**:1778-1785. DOI: 10.1016/j.ophtha.2013.01.018
- [8] Werkmeister RM, Sapeta S, Schmidl D, Garhöfer G, Schmidinger G, Aranha Dos Santos V, Aschinger GC, Baumgartner I, Pircher N, Schwarzhans F, Pantalon A, Dua H, Schmetterer L. Ultrahigh-resolution OCT imaging of the human cornea. *Biomedical Optics Express*. 2017;**8**:1221-1239. DOI: 10.1364/BOE.8.001221
- [9] Doors M, Cruysberg LPJ, Berendschot TTJM, de BJ, Verbakel F, Webers CAB, Nuijts RMMA. Comparison of central corneal thickness and anterior chamber depth measurements using three imaging technologies in normal eyes and after phakic intraocular lens implantation. *Graefe's Archive for Clinical and Experimental Ophthalmology*. 2009;**247**:1139-1146. DOI: 10.1007/s00417-009-1086-6
- [10] Szalai E, Berta A, Hassan Z, Módis L. Reliability and repeatability of swept-source Fourier-domain optical coherence tomography and Scheimpflug imaging in keratoconus. *Journal of Cataract and Refractive Surgery*. 2012;**38**:485-494. DOI: 10.1016/j.jcrs.2011.10.027
- [11] Schröder S, Mäurer S, Eppig T, Seitz B, Rubly K, Langenbucher A. Comparison of corneal tomography: Repeatability, precision, misalignment, mean elevation, and mean Pachymetry. *Current Eye Research*. 2018:1-8. DOI: 10.1080/02713683.2018.1441873

- [12] Grieve K, Georgeon C, Andreiuolo F, Borderie M, Ghoubay D, Rault J, Borderie VM. Imaging microscopic features of Keratoconic corneal morphology. *Cornea*. 2016;**35**:1621-1630. DOI: 10.1097/ICO.0000000000000979
- [13] Abou Shousha M, Perez VL, Fraga Santini Canto AP, Vaddavalli PK, Sayyad FE, Cabot F, Feuer WJ, Wang J, Yoo SH. The use of Bowman's layer vertical topographic thickness map in the diagnosis of keratoconus. *Ophthalmology*. 2014;**121**:988-993. DOI: 10.1016/j.ophtha.2013.11.034
- [14] Pahuja N, Shroff R, Pahanpate P, Francis M, Veeboy L, Shetty R, Nuijts RMMA, Sinha Roy A. Application of high resolution OCT to evaluate irregularity of Bowman's layer in asymmetric keratoconus. *Journal of Biophotonics*. 2017;**10**:701-707. DOI: 10.1002/jbio.201600106
- [15] Pircher N, Schwarzhans F, Holzer S, Lammer J, Schmidl D, Bata AM, Werkmeister RM, Seidel G, Garhöfer G, Gschließer A, Schmetterer L, Schmidinger G. Distinguishing keratoconic eyes and healthy eyes using ultrahigh-resolution (UHR)-OCT based corneal epithelium thickness mapping. *American Journal of Ophthalmology*. DOI: 10.1016/j.ajo.2018.02.006
- [16] Seitz B, Cursiefen C, El-Husseiny M, Viestenz A, Langenbucher A, Szentmáry N. DALK und perforierende Laserkeratoplastik bei fortgeschrittenem Keratokonus. *Der Ophthalmologe*. 2013;**110**:839-848. DOI: 10.1007/s00347-013-2822-1
- [17] Kucumen BR, Yenerel NM, Gorgun E, Dinc UA. Anterior segment optical coherence tomography findings of acute hydrops in a patient with keratoconus. *Ophthalmic Surgery, Lasers and Imaging*. 2010;**41**(Suppl):S114-S116. DOI: 10.3928/15428877-20101031-12
- [18] Yahia Chérif H, Gueudry J, Afriat M, Delcampe A, Attal P, Gross H, Muraine M. Efficacy and safety of pre-Descemet's membrane sutures for the management of acute corneal hydrops in keratoconus. *The British Journal of Ophthalmology*. 2015;**99**:773-777. DOI: 10.1136/bjophthalmol-2014-306287
- [19] Siebelmann S, Steven P, Cursiefen C. Intraoperative optische Kohärenztomografie bei der tiefen anterioren lamellären Keratoplastik. *Klinische Monatsblätter für Augenheilkunde*. 2016;**233**:717-721. DOI: 10.1055/s-0042-108588
- [20] De Benito-Llopis L, Mehta JS, Angunawela RI, Ang M, Tan DTH. Intraoperative anterior segment optical coherence tomography: A novel assessment tool during deep anterior lamellar keratoplasty. *American Journal of Ophthalmology*. 2014;**157**:334-341.e3. DOI: 10.1016/j.ajo.2013.10.001
- [21] Fu D, Wang L, Zhou X-T, Yu Z-Q. Cap morphology after small-incision lenticule extraction and its effects on intraocular scattering. *International Journal of Ophthalmology*. 2018;**11**:456-461. DOI: 10.18240/ijo.2018.03.16
- [22] Urkude J, Titiyal JS, Sharma N. Intraoperative optical coherence tomography-guided Management of cap-Lenticule Adhesion during SMILE. *Journal of Refractive Surgery*. 2017;**33**:783-786. DOI: 10.3928/1081597X-20170920-01

- [23] Titiyal JS, Rathi A, Kaur M, Falera R. AS-OCT as a rescue tool during difficult lenticle extraction in SMILE. *Journal of Refractive Surgery*. 2017;**33**:352-354. DOI: 10.3928/1081597X-20170216-01
- [24] Monteiro T, Alfonso JF, Franqueira N, Faria-Correia F, Ambrósio R, Madrid-Costa D. Predictability of tunnel depth for intrastromal corneal ring segments implantation between manual and femtosecond laser techniques. *Journal of Refractive Surgery*. 2018;**34**:188-194. DOI: 10.3928/1081597X-20180108-01
- [25] Vega-Estrada A, Alio JL. The use of intracorneal ring segments in keratoconus. *Eye and vision (London, England)*. 2016;**3**:8. DOI: 10.1186/s40662-016-0040-z
- [26] El-Husseiny M, Tsintarakis T, Eppig T, Langenbucher A, Seitz B. Intrakorneale Ringsegmente beim Keratokonus. *Der Ophthalmologe*. 2013;**110**:823-6, 828-9. DOI: 10.1007/s00347-013-2821-2
- [27] Zirm E. Eine erfolgreiche totale Keratoplastik. *Graefe's Archive for Clinical and Experimental Ophthalmology*. 1906;**64**:580-593
- [28] Ono T, Ishiyama S, Hayashidera T, Mori Y, Nejima R, Miyata K, Amano S. Twelve-year follow-up of penetrating keratoplasty. *Japanese Journal of Ophthalmology*. 2017;**61**:131-136. DOI: 10.1007/s10384-016-0489-2
- [29] Szentmáry N, Langenbucher A, Naumann GOH, Seitz B. Intra-individual variability of penetrating keratoplasty outcome after excimer laser versus motorized corneal trephination. *Journal of Refractive Surgery*. 2006;**22**:804-810
- [30] Sung MS, Yoon KC. Evaluation of graft-host interface after penetrating keratoplasty using anterior segment optical coherence tomography. *Japanese Journal of Ophthalmology*. 2014;**58**:282-289. DOI: 10.1007/s10384-014-0309-5
- [31] Seitz B, Langenbucher A, Hager T, Janunts E, El-Husseiny M, Szentmáry N. Penetrating keratoplasty for keratoconus - Excimer versus femtosecond laser trephination. *The Open Ophthalmology Journal*. 2017;**11**:225-240. DOI: 10.2174/1874364101711010225
- [32] Yenerel NM, Kucumen RB, Gorgun E. The complementary benefit of anterior segment optical coherence tomography in penetrating keratoplasty. *Clinical Ophthalmology*. 2013;**7**:1515-1523. DOI: 10.2147/OPHTH.S45904
- [33] Melles GRJ, Eggink FAGJ, Lander F, Pels E, Rietveld FJR, Beekhuis WH, Binder PS. A surgical technique for posterior lamellar keratoplasty. *Cornea*. 1998;**17**:618. DOI: 10.1097/00003226-199811000-00010
- [34] Melles GRJ, Wijdh RHJ, Nieuwendaal CP. A technique to excise the Descemet membrane from a recipient cornea (descemetorhexis). *Cornea*. 2004;**23**:286-288. DOI: 10.1097/00003226-200404000-00011
- [35] Steverink JG, Wisse RPL. Intraoperative optical coherence tomography in descemet stripping automated endothelial keratoplasty: pilot experiences. *International Ophthalmology*. 2017;**37**:939-944. DOI: 10.1007/s10792-016-0338-9

- [36] Kobayashi A, Yokogawa H, Mori N, Sugiyama K. Visualization of pre-cut DSAEK and pre-stripped DMEK donor corneas by intraoperative optical coherence tomography using the RESCAN 700. *BMC Ophthalmology*. 2016;**16**:135. DOI: 10.1186/s12886-016-0308-z
- [37] Koenig SB, Covert DJ, Dupps WJ, Meisler DM. Visual acuity, refractive error, and endothelial cell density six months after Descemet stripping and automated endothelial keratoplasty (DSAEK). *Cornea*. 2007;**26**:670-674. DOI: 10.1097/ICO.0b013e3180544902
- [38] Bahar I, Kaiserman I, Livny E, Slomovic A, Slomovic A. Changes in corneal curvatures and anterior segment parameters after descemet stripping automated endothelial keratoplasty. *Current Eye Research*. 2010;**35**:961-966. DOI: 10.3109/02713683.2010.506967
- [39] Langenbacher A, Szentmáry N, Spira C, Seitz B, Eppig T. Hornhautbrechwert nach 'Descemet Stripping Automated Endothelial Keratoplasty' (DSAEK) - Modellierung und Konzept für die Berechnung von Intraokularlinsen. *Zeitschrift für Medizinische Physik*. 2016;**26**:120-126. DOI: 10.1016/j.zemedi.2015.02.003
- [40] Melles GRJ, Ong TS, Ververs B, van der Wees J. Descemet membrane endothelial keratoplasty (DMEK). *Cornea* 2006;**25**:987-990. DOI: 10.1097/01.icc.0000248385.16896.34
- [41] Flockerzi E, Maier P, Böhringer D, Reinshagen H, Kruse F, Cursiefen C, Reinhard T, Geerling G, Torun N, Seitz B. Trends in corneal transplantation from 2001 to 2016 in Germany: a report of the DOG-section cornea and its keratoplasty registry. *American Journal of Ophthalmology*. 2018;**188**:91-98. DOI: 10.1016/j.ajo.2018.01.018
- [42] Röck T, Bartz-Schmidt KU, Röck D, Yoeruek E. Refraktionsänderung nach der Descemet-Membran-Endothelkeratoplastik. *Der Ophthalmologe*. 2014;**111**:649-653. DOI: 10.1007/s00347-013-2939-2
- [43] Girbardt C, Oertel N, Adamek-Dyk J, Wiedemann P, Nestler A. Refraktive Veränderungen bei Triple-Descemet-Membran-Endothel-Keratoplastik. *Der Ophthalmologe*. 2016;**113**:217-222. DOI: 10.1007/s00347-015-0201-9
- [44] Wolf AH, Neubauer AS, Priglinger SG, Kampik A, Welge-Luessen UC. Detection of laser in situ keratomileusis in a postmortem eye using optical coherence tomography. *Journal of Cataract and Refractive Surgery*. 2004;**30**:491-495. DOI: 10.1016/j.jcrs.2003.06.007
- [45] Neubauer AS, Priglinger SG, Thiel MJ, May C-A, Welge-Lüssen UC. Sterile structural imaging of donor cornea by optical coherence tomography. *Cornea*. 2002;**21**:490-494
- [46] Priglinger SG, Neubauer AS, May C-A, Alge CS, Wolf AH, Mueller A, Ludwig K, Kampik A, Welge-Luessen U. Optical coherence tomography for the detection of laser in situ keratomileusis in donor corneas. *Cornea*. 2003;**22**:46-50
- [47] Janunts E, Langenbacher A, Seitz B. In vitro corneal tomography of donor cornea using anterior segment OCT. *Cornea*. 2016;**35**:647-653. DOI: 10.1097/ICO.0000000000000761
- [48] Damian A, Seitz B, Langenbacher A, Eppig T. Optical coherence tomography-based topography determination of corneal grafts in eye bank cultivation. *Journal of Biomedical Optics*. 2017;**22**:16001. DOI: 10.1117/1.JBO.22.1.016001

- [49] Fernandes P, González-Méijome JM, Madrid-Costa D, Ferrer-Blasco T, Jorge J, Montés-Micó R. Implantable collamer posterior chamber intraocular lenses: A review of potential complications. *Journal of Refractive Surgery*. 2011;**27**:765-776. DOI:10.3928/1081597X-20110617-01
- [50] Fink AM, Gore C, Rosen E. Cataract development after implantation of the Staar Collamer posterior chamber phakic lens. *Journal of Cataract and Refractive Surgery*. 1999;**25**:278-282
- [51] Trindade F, Pereira F. Cataract formation after posterior chamber phakic intraocular lens implantation. *Journal of Cataract and Refractive Surgery*. 1998;**24**:1661-1663
- [52] Khalifa YM, Goldsmith J, Moshirfar M. Bilateral explantation of Visian implantable Collamer lenses secondary to bilateral acute angle closure resulting from a non-pupillary block mechanism. *Journal of Refractive Surgery*. 2010;**26**:991-994. DOI: 10.3928/1081597X-20100521-01
- [53] Bechmann M, Ullrich S, Thiel MJ, Kenyon KR, Ludwig K. Imaging of posterior chamber phakic intraocular lens by optical coherence tomography. *Journal of Cataract and Refractive Surgery*. 2002;**28**:360-363
- [54] Alfonso JF, Fernández-Vega L, Lisa C, Fernandes P, González-Meijome J, Montés-Micó R. Long-term evaluation of the central vault after phakic Collamer® lens (ICL) implantation using OCT. *Graefe's Archive for Clinical and Experimental Ophthalmology*. 2012;**250**:1807-1812. DOI: 10.1007/s00417-012-1957-0
- [55] Kojima T, Yokoyama S, Ito M, Horai R, Hara S, Nakamura T, Ichikawa K. Optimization of an implantable collamer lens sizing method using high-frequency ultrasound biomicroscopy. *American Journal of Ophthalmology*. 2012;**153**:632-7, 637.e1. DOI: 10.1016/j.ajo.2011.06.031
- [56] Nakamura T, Isogai N, Kojima T, Yoshida Y, Sugiyama Y. Implantable Collamer lens sizing method based on swept-source anterior segment optical coherence tomography. *American Journal of Ophthalmology*. 2018;**187**:99-107. DOI: 10.1016/j.ajo.2017.12.015
- [57] Tsintarakis T, Eppig T, Langenbacher A, Seitz B, El-Husseiny M. Kann die implantierbare Collamer-Linse mit Aquaport eine Winkelblockproblematik sicher verhindern? Erste Erfahrungen aus dem Homburger Zentrum für refraktive Chirurgie. *Der Ophthalmologe*. 2015;**112**:418-423. DOI: 10.1007/s00347-015-3237-y
- [58] Zhang J, Luo H-H, Zhuang J, Yu K-M. Comparison of anterior section parameters using anterior segment optical coherence tomography and ultrasound biomicroscopy in myopic patients after ICL implantation. *International Journal of Ophthalmology*. 2016;**9**: 58-62. DOI: 10.18240/ijo.2016.01.10